
Hybrid diffusion models: combining supervised and generative pretraining for label-efficient fine-tuning of segmentation models

Bruno Sauvalle
Mines Paris PSL University & EPFL*

Mathieu Salzmann
Swiss Data Science Center & EPFL

Abstract

We are considering in this paper the task of label-efficient fine-tuning of segmentation models: We assume that a large labeled dataset is available and allows to train an accurate segmentation model in one domain, and that we have to adapt this model on a related domain where only a few samples are available. We observe that this adaptation can be done using two distinct methods: The first method, supervised pretraining, is simply to take the model trained on the first domain using classical supervised learning, and fine-tune it on the second domain with the available labeled samples. The second method is to perform self-supervised pretraining on the first domain using a generic pretext task in order to get high-quality representations which can then be used to train a model on the second domain in a label-efficient way. We propose in this paper to fuse these two approaches by introducing a new pretext task, which is to perform simultaneously image denoising and mask prediction on the first domain. We motivate this choice by showing that in the same way that an image denoiser conditioned on the noise level can be considered as a generative model for the unlabeled image distribution using the theory of diffusion models, a model trained using this new pretext task can be considered as a generative model for the joint distribution of images and segmentation masks under the assumption that the mapping from images to segmentation masks is deterministic. We then empirically show on several datasets that fine-tuning a model pretrained using this approach leads to better results than fine-tuning a similar model trained using either supervised or unsupervised pretraining only.

1 Introduction

Image segmentation is one of the most fundamental computer vision tasks. Current state of the art segmentation models rely on supervised learning, which requires the availability of a large dataset of labeled data. However creating labeled data is far more difficult and expensive for segmentation than for image classification, since labeling a complete image requires to annotate the class of each pixel of this image. As a consequence, the development of label-efficient training methods, i.e. methods allowing to train a model using only a small number of labeled samples, has been the subject of numerous research works in the last decade.

One can distinguish two main approaches to handling this problem:

- The first method is called supervised pretraining: A segmentation model is first trained on a dataset where enough labeled data is available, and then fine-tuned on a different target dataset, where only a few labeled samples are available.

*Centre for Robotics, Mines Paris. Work conducted as a visiting professor at EPFL, Computer Vision Laboratory

- The second method, called unsupervised pretraining, is to assume that a large number of unlabeled data samples of the dataset of interest is available and to pretrain a model using these unlabeled samples to learn efficient representations, by leveraging various self-supervised learning strategy, and then to fine-tune the pretrained model using the available labeled samples.

We show in this paper that it is possible to fuse these two approaches. More precisely, we take our inspiration from recent works showing that UNets pretrained as unconditional diffusion models learn representations that can be label-efficient for segmentation in the classical semi-supervised setting, when only one domain is considered. In the setting considered in this paper, where sufficient labeled data is available in a first domain, and the model has to be adapted to a second domain where only a few samples are available, we propose to train a UNet simultaneously as a segmentation model and a diffusion model on the first domain before fine-tuning it on the second domain where the data is scarce. Our hypothesis is that the representations learnt using this process will be more efficient for segmentation fine-tuning than if the UNet is trained only as a diffusion model or as a supervised segmentation model.

The main contributions of this paper are the following:

- We introduce the concept of hybrid diffusion model and provide theoretical results showing that a trained hybrid diffusion model can be used both as a generative model for the joint distribution of the images and associated masks and as a supervised segmentation model.
- We provide experimental results showing that fine-tuning a pretrained hybrid diffusion model is more effective than fine-tuning a similar model pretrained using supervised or unsupervised pretraining alone.

2 Related work and background

Baranchuk et al. [2] and Rousseau et al. [34] showed that fine-tuning a pretrained class-unconditional diffusion model could give very good results for segmentation tasks when a few labeled samples are available in the classical semi-supervised setting where only one domain is considered. Both works rely on the ADM UNet architecture [11], which combines convolutional layers and global attention layers.

- Baranchuk et al. [2] proposed to freeze the UNet after pretraining. For fine-tuning, a separate MLP is trained in a pixel-wise manner to perform segmentation using as input the corresponding pixel feature map activations of the UNet for different time-steps, rescaled as necessary. Rosnati et al. [33] later showed that with this method, the smallest time-steps are the most informative and proposed to share MLP weights across time-steps to improve generalization. Li et al. [23] showed that although the diffusion models recommended for this method are large (554 M parameters), it is possible to distill these models into a smaller backbones without accuracy loss.
- Rousseau et al. [34] proposed to add a linear classification layer to a pretrained time-conditioned diffusion model with a fixed condition $t = 1$ and fine-tune it as a segmentation model. More recently, Huang et al. [16] proposed a similar method, but fine-tuning only the decoder of the diffusion model and not the encoder.

These results are consistent with numerous works [41, 42, 46, 48, 28], which have shown since 2008 that denoising is an effective pretext task for generic self-supervised learning. Prakash et al. [31], Buchholz et al. [4] and Wen et al. [45] showed that denoising is also an effective pretext task for segmentation. Brempong et al. [3] however found that combining a frozen pretrained encoder with denoising pretraining of the decoder was more effective than pretraining the whole model using denoising, except when the number of labeled samples available for fine-tuning is very low. The authors thus recommend to build a segmentation model using an encoder pretrained on Imagenet, keep it frozen, and then pretrain the decoder with denoising.

Numerous other self-supervised pretraining methods have also been developed for generic encoder pretraining and can be effective for segmentation tasks. Generative pretraining methods are not limited to denoising but also include masked autoencoding [15]. Discriminative methods such as SimCLR

[8], MoCo [14] or Dino [5] have also proven to be very effective but require to design manually the set of transformations that is used to build the different views of an image. These pretraining methods generally only allow to get low resolution feature maps, which may be suboptimal for segmentation tasks, but some pretext tasks for self-supervised learning have been specifically developed for dense prediction models such as pixel-wise contrastive learning [44].

Ng and Jordan [29] provided in 2001 theoretical justifications that training a model to learn the joint distribution $p(x, y)$ allows for label-efficient training. Raina et al. [32] introduced the expression "hybrid model" to designate models trained using both generative and discriminative targets. In the context of image classification, Khosla et al. [18], Su et al. [38] and Liang et al. [24] have proposed image encoder pretraining methods involving both self-supervised learning and supervised learning from image class labels. Closer to our work, Deja et al. [10] proposed to pretrain a shared encoder jointly for diffusion pretraining and supervised noisy image classification.

Several works have built joint generative models associated to segmentation datasets and studied their possible applications. Most of these works [40, 49, 22] proposed to use this joint generative model to produce new training samples, but Li et al. [21] built a GAN generative model for the joint distribution of images and masks, and showed that using the associated latent space could be effective for generalization and label-efficient learning.

Numerous works [50, 7, 25] have addressed the problem of adapting a segmentation model trained on one domain to another related domain. Except for fine-tuning the pretrained model on the available labeled samples, the methods developed for this task however generally assume that a large number of unlabeled samples is available in the target dataset.

3 Methodology

3.1 Hybrid diffusion models

Let us first recall why an image denoiser conditioned on the noise level can be considered as a generative model thanks to the theory of diffusion models. We follow the theoretical framework of Song et al. [36], the notations of Kingma et al. [19], and consider a discrete forward noising process x_0, x_1, \dots, x_T which, if T is large, can be identified with a stochastic process described by the stochastic differential equation

$$dx_t = f(t)x_t dt + g(t)dw, \quad (1)$$

with $q_t(x_t|x_0) = \mathcal{N}(x_t|\alpha_t x_0, \sigma_t^2 I)$ and $f(t) = \frac{d \log \alpha_t}{dt}$, $g^2(t) = \frac{d\sigma_t^2}{dt} - 2 \frac{d \log \alpha_t}{dt} \sigma_t^2$.

The associated reverse SDE [1] is

$$dx_t = [f(t)x_t - g(t)^2 \nabla_{x_t} \log(p(x_t))]dt + g(t)d\bar{w}, \quad (2)$$

where $d\bar{w}$ refers to a reverse brownian motion.

The quantity $\nabla_{x_t} \log(p(x_t))$ can be learnt from the data thanks to Tweedie's formula [12], which leads to the equality

$$\nabla_{x_t} \log(p(x_t)) = \frac{\alpha_t \mathbb{E}[x_0|x_t] - x_t}{\sigma_t^2}. \quad (3)$$

As a consequence, the reverse SDE can be written as

$$dx_t = [f(t)x_t - g(t)^2 \left(\frac{\alpha_t \mathbb{E}[x_0|x_t] - x_t}{\sigma_t^2} \right)]dt + g(t)d\bar{w}, \quad (4)$$

and the associated probability flow [36] can be described by the ODE

$$dx_t = [f(t)x_t - \frac{g(t)^2}{2} \left(\frac{\alpha_t \mathbb{E}[x_0|x_t] - x_t}{\sigma_t^2} \right)]dt. \quad (5)$$

Training a denoiser conditioned on the noise level or on t using an MSE loss provides an estimator of $\mathbb{E}[x_0|x_t]$ and allows one to get a complete description of the reverse SDE or ODE. Assuming that α_T is small compared to σ_T so that $p(x_T)$ can be identified with pure Gaussian noise, it is then possible

to generate samples from the distribution $p(x)$ by sampling x_T from a Gaussian distribution and then solving the equation 4 or 5 using an SDE or ODE solver.

Let us now consider a dataset composed of pairs $z_i = (x_i, y_i)$, where the x_i are i.i.d. following some unknown distribution $p(x)$, and y is a deterministic unknown function of x , $y = \mu(x)$. In this paper, x will be an image that we want to analyse and y the associated segmentation mask.

We propose to train a denoiser conditioned on t to provide an estimate of x and y from a noisy version x_t of x only. If we assume that we train this denoiser with an MSE loss, the denoiser provides an estimator of $\mathbb{E}[z|x_t] = \mathbb{E}[x, y|x_t]$.

This denoiser can be trivially used to generate samples from the distribution $p(x, y)$ by first using the x estimates $\mathbb{E}[x|x_t]$ of the denoiser to generate samples from the distribution $p(x)$ using the associated ODE or SDE, and then using the denoiser at step zero to predict y from x , since for $t = 0$ (no noise), the trained denoiser provides an estimate of $\mathbb{E}[y|x] = \mu(x)$

It appears however than we can also generate samples from the joint distribution $p(x, y)$ by solving a reverse SDE or ODE involving this denoiser, which is formally fully similar to the reverse SDE or ODE of diffusion models described above. More precisely, we have the following proposition for the SDE:

Proposition 1 *Let us assume that x_T is sampled from a normal Gaussian distribution and y_T is set to any arbitrary value, and let $z_t = (x_t, y_t)$. Then, solving the reverse SDE*

$$dz_t = [f(t)z_t - g(t)^2 \left(\frac{\alpha_t \mathbb{E}[z|x_t] - z_t}{\sigma_t^2} \right)] dt + g(t) d\bar{w} \quad (6)$$

allows one to obtain samples from the distribution $p(z) = p(x, y)$ for $t = 0$.

It can be noted that equation 6 is exactly the same as equation 4 except that the expectation term is $\mathbb{E}[z|x_t]$ and not $\mathbb{E}[z|z_t]$. We have a similar result for the probability flow ODE:

Proposition 2 *Let us assume that x_T is sampled from a normal Gaussian distribution and y_T is set to any arbitrary value, and let $z_t = (x_t, y_t)$. Then solving the ODE*

$$dz_t = [f(t)z_t - \frac{g(t)^2}{2} \left(\frac{\alpha_t \mathbb{E}[z|x_t] - z_t}{\sigma_t^2} \right)] dt$$

allows to obtain samples from the distribution $p(x, y)$ for $t = 0$.

The proofs of these propositions are provided in the supplementary material.

One may intuitively apprehend Proposition 2 by considering that the ODE associated to standard diffusion models provides a mapping between data samples (x, y) and latent variables (x_T, y_T) following a Gaussian distribution. If y is a deterministic function of x , this leads to an unnecessary increase of the dimensionality of the latent space compared to the dimensionality of the data manifold. Proposition 2 shows that it is possible to avoid this augmentation by reducing the dimensionality of the latent space to the dimensionality of the image space.

We then call a noise conditional model providing an estimate of $\mathbb{E}[z|x_t] = \mathbb{E}[x, y|x_t]$ a hybrid diffusion model: It can be considered both as a generative model for the joint distribution $p(z) = p(x, y)$, but also, taking $t = 0$, as a pure discriminative segmentation model.

3.2 Using hybrid diffusion models for representation learning

Considering that noise-conditioned denoisers used for diffusion models have shown to be effective representation learners in the unsupervised setting, we expect a hybrid diffusion model to also be effective for representation learning. Since the hybrid diffusion model has learned the full joint distribution of the segmentation dataset, we expect the representations learned by a hybrid diffusion model to be more effective than those learned using pure unsupervised learning or pure supervised learning.

To perform label-efficient transfer learning, we then propose to first train a hybrid diffusion model on a first domain where we have a lot of labeled samples, and then fine-tune it on a second domain, where only a few samples are available. The architecture of a hybrid diffusion model is the same as a

standard unconditional diffusion model, with the exception that the number of output channels has to be extended for color images from 3 to $3 + K$, where K is the number of segmentation classes since we use one-hot encoding for the segmentation masks.

We use the same standard MSE loss function as in [35] except that we have found from our experiments that it is necessary to insert a weighting factor λ to give a significantly lower weight to the segmentation masks reconstruction loss. If x, y are the ground-truth images and masks and \hat{x}, \hat{y} the predicted images and masks, the loss function is then

$$\mathcal{L}(x, y, \hat{x}, \hat{y}, t) = \frac{\alpha_t^2}{\sigma_t^2} \left(\frac{1}{3hw} \|x - \hat{x}\|^2 + \frac{1}{Khw} \lambda \|y - \hat{y}\|^2 \right),$$

where h, w are the height and width of the image and K is the number of segmentation classes.

We will investigate the two fine-tuning techniques that have been introduced in 2 and have proven to be effective for diffusion models:

- The first one, which we will call vanilla fine-tuning, is to freeze the condition $t = 1$ and perform a supervised fine-tuning of this model considered as a segmentation model using the labeled samples of the second domain. This can be considered as a straightforward extension of the PTDR fine-tuning method proposed in [34]. If the number of classes of the second dataset is not the same as the number of classes in the first domain, we replace the last layer of the UNet by a new layer with the correct number of output channels, initialized randomly.
- We also adapt the LEDM method [2] to hybrid diffusion models, which is also straightforward since the model we use has the same architecture [11]: We freeze the model after pretraining and train a pixel-wise MLP to perform segmentation using as input the feature map activations of the model for different time-steps, rescaled as necessary to the input image size.

4 Experiments

4.1 Datasets

We consider the following segmentation datasets:

- Skin lesion segmentation: We use the ISIC 2018 dataset for pretraining and the DermIS and PH2 datasets for fine-tuning.
- Chest X-ray segmentation: We use the Shenzhen dataset for pretraining and the NIH and Montgomery datasets for fine-tuning.
- Face segmentation: We use the Celebamask-HQ dataset for pretraining and FFHQ 34 for fine-tuning. It should be noted that while these datasets are closely related (they both show human faces), they do not use the same classes.

The main characteristics of these datasets are listed in Table 4.1 and samples of each dataset are provided in the supplementary material.

We use the full datasets for unsupervised or hybrid pretraining, but only 20 images as training set for fine-tuning, the remaining being used for validation and testing.

For skin lesion datasets, we do not perform any preprocessing except rescaling to 256×256 . For Celebamask-HQ, we observe that the provided masks overlap since the "skin" masks cover the whole face. We then convert the provided masks into non overlapping masks by giving the skin class a lower priority compared to the other classes. For chest X-ray datasets, we perform histogram equalization and gamma correction as in Oh et al. [30] and convert the one channel images to three channel images by duplicating each channel.

We do not perform any data augmentation on the fine-tuning datasets since our goal is to study the behavior of our model in the low data regime. On ISIC 2018, we use horizontal and vertical flips. Considering the small size of the Shenzhen dataset and the fact that horizontal or vertical flips would obviously lead to out of distribution samples, we perform limited random cropping: The coordinates

Dataset	used for	number of samples	number of classes	data augmentation
ISIC 2018 [9]	pretraining	2594	2	horizontal and vertical flip
DermIS [13]	fine-tuning	69	2	no
PH2 [27]	fine-tuning	200	2	no
Shenzhen [17, 37]	pretraining	566	2	random cropping
NIH [39]	fine-tuning	100	2	no
Montgomery [37]	fine-tuning	138	2	no
CelebaMask-HQ [20]	pretraining	30000	19	no
FFHQ-34 [2]	fine-tuning	40	34	no

Table 1: Main characteristics of the datasets used in our evaluation.

of the cropped rectangles are randomly picked at a horizontal or vertical distance to the border of the original image from 0% to 5% of the image size before rescaling to 256×256 (Some augmented samples are provided in the supplementary material).

4.2 Methods

We use ADM [11]² as UNet architecture for the diffusion model. This choice is motivated by the fact that the LEDM method is designed to use the feature maps of this model.

To limit training costs for this preliminary study, we significantly depart from the settings recommended in [11] and also implemented in [2]: We reduce the number of channels of the model from 256 to 128, reducing the number of parameters of the model from 554 M to 138 M parameters. The number of iterations during pretraining is set to 40'000 with a batch size of 64 for ISIC 2018 and Shenzhen, and 90'000 with a batch size of 64 for Celabamask-HQ, instead of the range 200K-500K with a batch size of 256 recommended in [11].

We pretrain the models using the Hugging Face diffusers framework [43], using the AdamW optimizer with a constant learning rate of 10^{-4} and 2000 linear warm-up steps.

For the fine-tuning phase, we use the cross-entropy loss, a batch size of 12 and a learning rate of $2 \cdot 10^{-4}$. We evaluate the model on the validation set at the end of each epoch using the target metric and stop the training when no improvement is obtained during 20 epochs, keeping the model with the best evaluation score. The results provided are averages over three fine-tuning runs.

For the implementation of the LEDM fine-tuning technique, we use the official code base³. We perform the tests with 1 MLP and do not engage in any hyperparameter optimization.

For medical segmentation datasets, we use the average Jaccard index as evaluation metric (average of foreground class IoU per sample). For the face segmentation datasets, we use the average mIoU per class, following [2].

λ is set to $1 \cdot 10^{-4}$ following preliminary tests with $\lambda \in \{1, 10^{-1}, 10^{-2}, 10^{-3}, 10^{-4}, 10^{-5}\}$.

Other experimental settings and hyperparameters are detailed in the supplementary material.

4.3 Results and discussion

Some samples generated using the proposed hybrid diffusion models are provided in the supplementary material and show that the trained hybrid models are genuine generative models.

To assess the performance of the proposed scheme for fine-tuning, we also fine-tune segmentation models on the same fine-tuning datasets according to the following scenarios:

²<https://github.com/openai/guided-diffusion>

³<https://github.com/yandex-research/ddpm-segmentation>

- training an ADM UNet with random initialization on the fine-tuning datasets (no pretraining at all).
- training a Deeplabv3 model [6] with ResNet-50 backbone pretrained on Imagenet 1K
- training a Segformer[47] B3 model with Mit encoder pretrained⁴ on Imagenet 1K
- pretraining a diffusion model using the images of the pretraining dataset and fine-tuning with the fine-tuning datasets using the LEDM method
- pretraining a diffusion model using the images of the pretraining dataset and fine-tuning with the fine-tuning datasets using vanilla fine-tuning
- pretraining a hybrid diffusion model using the methodology described in this paper and fine-tuning it using the LEDM method
- pretraining a hybrid diffusion model using the methodology described in this paper and fine-tuning it using vanilla fine-tuning
- training a Deeplabv3 model with ResNet-50 backbone pretrained on Imagenet 1K with the pretraining dataset, then fine-tuning it with the fine-tuning dataset
- training a Segformer B3 model with Mit encoder pretrained on Imagenet 1K with the pretraining dataset, then fine-tuning it with the fine-tuning dataset

The results of these evaluations are shown in Table 4.3.

One can observe that when no specific pretraining dataset is available, the models using encoders pretrained on Imagenet generally give significantly better results than the ADM UNet with random initialization.

Unsupervised pretraining the ADM UNet as a diffusion model gives a significant boost to the fine-tuning results, confirming the effectiveness of the methods proposed in [2] and [34].

Supervised pretraining followed by vanilla fine-tuning also allows to improve the results compared to random initialization, which was also expected, but using the LEDM fine-tuning method with an ADM UNet pretrained using supervised training does not seem to be effective.

Concerning the results of the hybrid diffusion model proposed in this paper, we observe that the LEDM fine-tuning method is also not effective, except for the FFHQ 34 dataset, which is consistent with the results observed for supervised pretraining.

We observe however that vanilla fine-tuning of the proposed hybrid diffusion model always gives better average results compared to supervised pretraining or unsupervised pretraining, with significant improvements on the DermIS and FFHQ 34 datasets.

Finally, we note that the results of vanilla fine-tuning our proposed hybrid diffusion model are competitive with, or superior to, those of the DeepLabv3 and SegFormer B3 models pretrained on both ImageNet-1K and the pretraining datasets.

	pretraining dataset fine-tuning dataset metric	ISIC 2018 PH2 20 samples Jaccard index	ISIC 2018 DermIS 20 samples Jaccard index	Shenzhen NIH 20 Jaccard index	Shenzhen Montgomery 20 Jaccard index	CelebaMask-HQ FFHQ-34 20 samples average of class IoU
no pretraining	ADM UNet	84.53 ±0.68	75.74 ±0.41	73.42 ±2.41	91.70 ±2.19	32.95 ±0.94
Imagenet 1K pretraining	Deeplabv3 model R50	82.89 ±0.83	73.89 ±4.16	90.54 ±0.42	93.97 ±0.13	40.00 ±1.16
	Segformer B3 model	86.01 ±0.94	86.63 ±1.06	91.19 ±0.48	94.90 ±0.29	46.52 ±0.33
unsupervised pretraining	LEDM on diffusion model	86.07	81.83	87.03	90.94	54.44
	fine-tuning of diffusion model	85.08 ±0.63	79.67 ±2.43	87.65 ±0.45	94.31 ±0.44	55.08 ±0.25
pretraining on labeled dataset	LEDM on supervised ADM Unet	84.09	78.01	89.33	91.46	45.66
	fine-tuning of supervised ADM UNet	87.94 ±0.42	81.45 ±0.16	90.68 ±1.86	94.54 ±1.23	54.49 ±0.63
	LEDM on hybrid model	85.43	78.16	85.92	90.71	56.59
	fine-tuning of hybrid model	88.23 ±0.21	86.76 ±1.04	92.17 ±0.45	95.45 ±0.11	56.91 ±0.56
1K pretraining + supervised pre-training	fine-tuning of supervised Segformer model	87.74 ±0.37	88.28 ±0.17	92.36 ±0.10	95.66 ±0.19	51.06 ±0.27
	fine-tuning of supervised Deeplabv3 model	89.44 ±0.36	86.50 ±0.46	92.22 ±0.14	95.55 ±0.05	47.32 ±0.37

Table 2: Empirical results.

⁴<https://huggingface.co/nvidia/mit-b3>

5 Conclusion

We have introduced in this paper the notion of hybrid diffusion model and provided experimental evidences that vanilla fine-tuning of such a model can be more effective than fine-tuning a similar supervised model or pretrained diffusion model. Further work is needed to explore the full potential of this new paradigm, but the preliminary experimental results described in this paper show that it allows one to benefit simultaneously from both supervised and unsupervised pretraining for segmentation tasks, which seems to be a natural requirement in many situations where labeled data is available in one domain and we are interested to adapt a model to a new domain where only a few samples are available.

References

- [1] Brian D.O. Anderson. Reverse-time diffusion equation models. *Stochastic Processes and their Applications*, 12(3):313–326, May 1982. ISSN 03044149. doi: 10.1016/0304-4149(82)90051-5.
- [2] Dmitry Baranchuk, Andrey Voynov, Ivan Rubachev, Valentin Khrukov, and Artem Babenko. Label-Efficient Semantic Segmentation with Diffusion Models. In *International Conference on Learning Representations*, October 2021.
- [3] Emmanuel Asiedu Brempong, Simon Kornblith, Ting Chen, Niki Parmar, Matthias Minderer, and Mohammad Norouzi. Denoising Pretraining for Semantic Segmentation. In *2022 IEEE/CVF Conference on Computer Vision and Pattern Recognition Workshops (CVPRW)*, pages 4174–4185, New Orleans, LA, USA, June 2022. IEEE. ISBN 978-1-66548-739-9. doi: 10.1109/CVPRW56347.2022.00462.
- [4] Tim-Oliver Buchholz, Mangal Prakash, Deborah Schmidt, Alexander Krull, and Florian Jug. DenoiSeg: Joint denoising and segmentation. In Adrien Bartoli and Andrea Fusiello, editors, *Computer Vision – ECCV 2020 Workshops*, pages 324–337, Cham, 2020. Springer International Publishing. ISBN 978-3-030-66415-2.
- [5] Mathilde Caron, Hugo Touvron, Ishan Misra, Herve Jegou, Julien Mairal, Piotr Bojanowski, and Armand Joulin. Emerging Properties in Self-Supervised Vision Transformers. In *2021 IEEE/CVF International Conference on Computer Vision (ICCV)*, pages 9630–9640, Montreal, QC, Canada, October 2021. IEEE. ISBN 978-1-66542-812-5. doi: 10.1109/ICCV48922.2021.00951.
- [6] Liang-Chieh Chen, George Papandreou, Florian Schroff, and Hartwig Adam. Rethinking atrous convolution for semantic image segmentation. *ArXiv*, abs/1706.05587, 2017.
- [7] Minghao Chen, Hongyang Xue, and Deng Cai. Domain adaptation for semantic segmentation with maximum squares loss. *2019 IEEE/CVF International Conference on Computer Vision (ICCV)*, pages 2090–2099, 2019.
- [8] Ting Chen, Simon Kornblith, Mohammad Norouzi, and Geoffrey Hinton. A simple framework for contrastive learning of visual representations. In Hal Daumé III and Aarti Singh, editors, *Proceedings of the 37th International Conference on Machine Learning*, volume 119 of *Proceedings of Machine Learning Research*, pages 1597–1607. PMLR, 2020-07-13/2020-07-18.
- [9] Noel C. F. Codella, David Gutman, M. Emre Celebi, Brian Helba, Michael A. Marchetti, Stephen W. Dusza, Aadi Kallou, Konstantinos Liopyris, Nabin Mishra, Harald Kittler, and Allan Halpern. Skin lesion analysis toward melanoma detection: A challenge at the 2017 International symposium on biomedical imaging (ISBI), hosted by the international skin imaging collaboration (ISIC). In *2018 IEEE 15th International Symposium on Biomedical Imaging (ISBI 2018)*, pages 168–172, Washington, DC, April 2018. IEEE. ISBN 978-1-5386-3636-7. doi: 10.1109/ISBI.2018.8363547.
- [10] Kamil Deja, Tomasz Trzciński, and Jakub M. Tomczak. Learning data representations with joint diffusion models. In Danai Koutra, Claudia Plant, Manuel Gomez Rodriguez, Elena Baralis, and Francesco Bonchi, editors, *Machine Learning and Knowledge Discovery in Databases: Research Track*, pages 543–559, Cham, 2023. Springer Nature Switzerland. ISBN 978-3-031-43415-0.

- [11] Prafulla Dhariwal and Alexander Nichol. Diffusion models beat gans on image synthesis. In M. Ranzato, A. Beygelzimer, Y. Dauphin, P.S. Liang, and J. Wortman Vaughan, editors, *Advances in Neural Information Processing Systems*, volume 34, pages 8780–8794. Curran Associates, Inc., 2021.
- [12] Bradley Efron. Tweedie’s Formula and Selection Bias. *Journal of the American Statistical Association*, 106(496):1602–1614, December 2011. ISSN 0162-1459, 1537-274X. doi: 10.1198/jasa.2011.tm11181.
- [13] Jeffrey Luc Glaister. Automatic segmentation of skin lesions from dermatological photographs. *Master’s thesis, University of Waterloo, Ontario, Canada*, 2013.
- [14] Kaiming He, Haoqi Fan, Yuxin Wu, Saining Xie, and Ross Girshick. Momentum contrast for unsupervised visual representation learning. In *2020 IEEE/CVF Conference on Computer Vision and Pattern Recognition (CVPR)*, pages 9726–9735, 2020. doi: 10.1109/CVPR42600.2020.00975.
- [15] Kaiming He, Xinlei Chen, Saining Xie, Yanghao Li, Piotr Dollar, and Ross Girshick. Masked autoencoders are scalable vision learners. In *Proceedings - 2022 IEEE/CVF conference on computer vision and pattern recognition, CVPR 2022*, Proceedings of the IEEE computer society conference on computer vision and pattern recognition, pages 15979–15988. IEEE Computer Society, 2022. doi: 10.1109/CVPR52688.2022.01553.
- [16] Yongzhi Huang, Jinxin Zhu, Haseeb Hassan, Liyilei Su, Jingyu Li, and Binding Huang. Label-efficient Multi-organ Segmentation Method with Diffusion Model, arXiv:2402.15216, February 2024.
- [17] Stefan Jaeger, Sema Candemir, Sameer Kiran Antani, Yi-Xiáng J Wáng, Pu-Xuan Lu, and George R. Thoma. Two public chest X-ray datasets for computer-aided screening of pulmonary diseases. *Quantitative imaging in medicine and surgery*, 4 6:475–7, 2014.
- [18] Prannay Khosla, Piotr Teterwak, Chen Wang, Aaron Sarna, Yonglong Tian, Phillip Isola, Aaron Maschinot, Ce Liu, and Dilip Krishnan. Supervised contrastive learning. In H. Larochelle, M. Ranzato, R. Hadsell, M.F. Balcan, and H. Lin, editors, *Advances in Neural Information Processing Systems*, volume 33, pages 18661–18673. Curran Associates, Inc., 2020.
- [19] Diederik Kingma, Tim Salimans, Ben Poole, and Jonathan Ho. Variational diffusion models. In M. Ranzato, A. Beygelzimer, Y. Dauphin, P.S. Liang, and J. Wortman Vaughan, editors, *Advances in Neural Information Processing Systems*, volume 34, pages 21696–21707. Curran Associates, Inc., 2021.
- [20] Cheng-Han Lee, Ziwei Liu, Lingyun Wu, and Ping Luo. MaskGAN: Towards Diverse and Interactive Facial Image Manipulation. In *2020 IEEE/CVF Conference on Computer Vision and Pattern Recognition (CVPR)*, pages 5548–5557, Seattle, WA, USA, June 2020. IEEE. ISBN 978-1-72817-168-5. doi: 10.1109/CVPR42600.2020.00559.
- [21] Daiqing Li, Junlin Yang, Karsten Kreis, Antonio Torralba, and Sanja Fidler. Semantic Segmentation with Generative Models: Semi-Supervised Learning and Strong Out-of-Domain Generalization. In *2021 IEEE/CVF Conference on Computer Vision and Pattern Recognition (CVPR)*, pages 8296–8307, Nashville, TN, USA, June 2021. IEEE. ISBN 978-1-66544-509-2. doi: 10.1109/CVPR46437.2021.00820.
- [22] Daiqing Li, Huan Ling, Seung Wook Kim, Karsten Kreis, Sanja Fidler, and Antonio Torralba. BigDatasetGAN: Synthesizing ImageNet with pixel-wise annotations. In *CVPR*, pages 21298–21308, 2022.
- [23] Daiqing Li, Huan Ling, Amlan Kar, David Acuna, Seung Wook Kim, Karsten Kreis, Antonio Torralba, and Sanja Fidler. DreamTeacher: Pretraining image backbones with deep generative models. In *Proceedings of the IEEE/CVF International Conference on Computer Vision (ICCV)*, pages 16698–16708, October 2023.
- [24] Feng Liang, Yangguang Li, and Diana Marculescu. SupMAE: Supervised Masked Autoencoders Are Efficient Vision Learners, January 2024.

- [25] Yuang Liu, Wei Zhang, and Jun Wang. Source-free domain adaptation for semantic segmentation. *2021 IEEE/CVF Conference on Computer Vision and Pattern Recognition (CVPR)*, pages 1215–1224, 2021.
- [26] Cheng Lu, Yuhao Zhou, Fan Bao, Jianfei Chen, Chongxuan LI, and Jun Zhu. DPM-solver: A fast ODE solver for diffusion probabilistic model sampling in around 10 steps. In S. Koyejo, S. Mohamed, A. Agarwal, D. Belgrave, K. Cho, and A. Oh, editors, *Advances in Neural Information Processing Systems*, volume 35, pages 5775–5787. Curran Associates, Inc., 2022.
- [27] Teresa Mendonca, Pedro M. Ferreira, Jorge S. Marques, Andre R. S. Marcal, and Jorge Rozeira. PH² - A dermoscopic image database for research and benchmarking. In *2013 35th Annual International Conference of the IEEE Engineering in Medicine and Biology Society (EMBC)*, pages 5437–5440, Osaka, July 2013. IEEE. ISBN 978-1-4577-0216-7. doi: 10.1109/EMBC.2013.6610779.
- [28] Soumik Mukhopadhyay, Matthew Gwilliam, Vatsal Agarwal, Namitha Padmanabhan, Archana Swaminathan, Srinidhi Hegde, Tianyi Zhou, and Abhinav Shrivastava. Diffusion models beat gans on image classification, arXiv: 2307.08702 [cs.CV], 2023.
- [29] Andrew Ng and Michael Jordan. On Discriminative vs. Generative Classifiers: A comparison of logistic regression and naive Bayes. In T. Dietterich, S. Becker, and Z. Ghahramani, editors, *Advances in Neural Information Processing Systems*, volume 14. MIT Press, 2001.
- [30] Yujin Oh, Sangjoon Park, and Jong Chul Ye. Deep Learning COVID-19 Features on CXR Using Limited Training Data Sets. *IEEE transactions on medical imaging*, 39(8):2688–2700, August 2020. ISSN 1558-254X. doi: 10.1109/TMI.2020.2993291.
- [31] Mangal Prakash, Tim-Oliver Buchholz, Manan Lalit, Pavel Tomancak, Florian Jug, and Alexander Krull. Leveraging Self-supervised Denoising for Image Segmentation. In *2020 IEEE 17th International Symposium on Biomedical Imaging (ISBI)*, pages 428–432, Iowa City, IA, USA, April 2020. IEEE. ISBN 978-1-5386-9330-8. doi: 10.1109/ISBI45749.2020.9098559.
- [32] Rajat Raina, Yirong Shen, Andrew McCallum, and Andrew Ng. Classification with hybrid generative/discriminative models. In S. Thrun, L. Saul, and B. Schölkopf, editors, *Advances in Neural Information Processing Systems*, volume 16. MIT Press, 2003.
- [33] Margherita Rosnati, Mélanie Roschewitz, and Ben Glocker. Robust semi-supervised segmentation with timestep ensembling diffusion models. In *Deep Generative Models for Health Workshop NeurIPS 2023*, 2023.
- [34] Jérémy Rousseau, Christian Alaka, Emma Covili, Hippolyte Mayard, Laura Misrachi, and Willy Au. Pre-training with diffusion models for dental radiography segmentation. In Anirban Mukhopadhyay, Ilkay Oksuz, Sandy Engelhardt, Dajiang Zhu, and Yixuan Yuan, editors, *Deep Generative Models*, pages 174–182, Cham, 2024. Springer Nature Switzerland. ISBN 978-3-031-53767-7.
- [35] Tim Salimans and Jonathan Ho. Progressive distillation for fast sampling of diffusion models. In *International Conference on Learning Representations*, 2022.
- [36] Yang Song, Jascha Sohl-Dickstein, Diederik P Kingma, Abhishek Kumar, Stefano Ermon, and Ben Poole. Score-based generative modeling through stochastic differential equations. In *International Conference on Learning Representations*, 2021.
- [37] Sergii Stirenko, Yuriy Kochura, Oleg Alienin, Oleksandr Rokovyi, Peng Gang, Wei Zeng, and Yuri Gordienko. Chest X-Ray Analysis of Tuberculosis by Deep Learning with Segmentation and Augmentation. In *2018 IEEE 38th International Conference on Electronics and Nanotechnology (ELNANO)*, pages 422–428, April 2018. doi: 10.1109/ELNANO.2018.8477564.
- [38] Weijie Su, Xizhou Zhu, Chenxin Tao, Lewei Lu, Bin Li, Gao Huang, Yu Qiao, Xiaogang Wang, Jie Zhou, and Jifeng Dai. Towards All-in-One Pre-Training via Maximizing Multi-Modal Mutual Information. In *2023 IEEE/CVF Conference on Computer Vision and Pattern Recognition (CVPR)*, pages 15888–15899, Vancouver, BC, Canada, June 2023. IEEE. ISBN 9798350301298. doi: 10.1109/CVPR52729.2023.01525.

- [39] Youbao Tang, Yuxing Tang, Jing Xiao, and Ronald M Summers. XLSor: A robust and accurate lung segmentor on chest x-rays using criss-cross attention and customized radiorealistic abnormalities generation. In *International Conference on Medical Imaging with Deep Learning (MIDL)*, 2019.
- [40] A Toker, M Eisenberger, D Cremers, and L Leal-Taixe. SatSynth: Augmenting image-mask pairs through diffusion models for aerial semantic segmentation. In *IEEE Conference on Computer Vision and Pattern Recognition (CVPR)*, 2024.
- [41] Pascal Vincent, Hugo Larochelle, Yoshua Bengio, and Pierre-Antoine Manzagol. Extracting and composing robust features with denoising autoencoders. In *Proceedings of the 25th International Conference on Machine Learning - ICML '08*, pages 1096–1103, Helsinki, Finland, 2008. ACM Press. ISBN 978-1-60558-205-4. doi: 10.1145/1390156.1390294.
- [42] Pascal Vincent, Hugo Larochelle, Isabelle Lajoie, Yoshua Bengio, and Pierre-Antoine Manzagol. Stacked denoising autoencoders: Learning useful representations in a deep network with a local denoising criterion. *Journal of Machine Learning Research*, 11:3371–3408, December 2010. ISSN 1532-4435.
- [43] Patrick von Platen, Suraj Patil, Anton Lozhkov, Pedro Cuenca, Nathan Lambert, Kashif Rasul, Mishig Davaadorj, Dhruv Nair, Sayak Paul, William Berman, Yiyi Xu, Steven Liu, and Thomas Wolf. Diffusers: State-of-the-art diffusion models, <https://github.com/huggingface/diffusers>, 2022.
- [44] Xinlong Wang, Rufeng Zhang, Chunhua Shen, Tao Kong, and Lei Li. Dense Contrastive Learning for Self-Supervised Visual Pre-Training. In *2021 IEEE/CVF Conference on Computer Vision and Pattern Recognition (CVPR)*, pages 3023–3032, Nashville, TN, USA, June 2021. IEEE. ISBN 978-1-66544-509-2. doi: 10.1109/CVPR46437.2021.00304.
- [45] R. Wen, H. Yuan, D. Ni, W. Xiao, and Y. Wu. From denoising training to test-time adaptation: Enhancing domain generalization for medical image segmentation. In *2024 IEEE/CVF Winter Conference on Applications of Computer Vision (WACV)*, pages 453–463, Los Alamitos, CA, USA, January 2024. IEEE Computer Society. doi: 10.1109/WACV57701.2024.00052.
- [46] Weilai Xiang, Hongyu Yang, Di Huang, and Yunhong Wang. Denoising Diffusion Autoencoders are Unified Self-supervised Learners. In *2023 IEEE/CVF International Conference on Computer Vision (ICCV)*, pages 15756–15766, Paris, France, October 2023. IEEE. ISBN 9798350307184. doi: 10.1109/ICCV51070.2023.01448.
- [47] Enze Xie, Wenhai Wang, Zhiding Yu, Anima Anandkumar, Jose M. Alvarez, and Ping Luo. SegFormer: Simple and efficient design for semantic segmentation with transformers. In M. Ranzato, A. Beygelzimer, Y. Dauphin, P.S. Liang, and J. Wortman Vaughan, editors, *Advances in Neural Information Processing Systems*, volume 34, pages 12077–12090. Curran Associates, Inc., 2021.
- [48] Zunzhi You, Daochang Liu, Bohyung Han, and Chang Xu. Beyond pretrained features: Noisy image modeling provides adversarial defense. In *Thirty-Seventh Conference on Neural Information Processing Systems*, 2023.
- [49] Y. Zhang, H. Ling, J. Gao, K. Yin, J. Lafleche, A. Barriuso, A. Torralba, and S. Fidler. DatasetGAN: Efficient labeled data factory with minimal human effort. In *2021 IEEE/CVF Conference on Computer Vision and Pattern Recognition (CVPR)*, pages 10140–10150, Los Alamitos, CA, USA, June 2021. IEEE Computer Society. doi: 10.1109/CVPR46437.2021.01001.
- [50] Yang Zou, Zhiding Yu, B. V. K. Vijaya Kumar, and Jinsong Wang. Unsupervised domain adaptation for semantic segmentation via class-balanced self-training. In Vittorio Ferrari, Martial Hebert, Cristian Sminchisescu, and Yair Weiss, editors, *Computer Vision – ECCV 2018*, pages 297–313, Cham, 2018. Springer International Publishing. ISBN 978-3-030-01219-9.

A Supplementary material

A.1 Proofs

Since propositions 1 and 2 are already known for classical diffusion models, we only prove the propositions for y_t and assume that the reverse ODE or SDE applied to x_t allows to sample x_0 values from the distribution $p(x)$.

We recall that

$$f(t) = \frac{d \log \alpha_t}{dt}$$

and

$$g^2(t) = \frac{d\sigma_t^2}{dt} - 2\frac{d \log \alpha_t}{dt} \sigma_t^2 = 2\sigma_t^2 \frac{d}{dt} \log\left(\frac{\sigma_t}{\alpha_t}\right)$$

A.1.1 Proof of proposition 1 (reverse SDE)

We consider the reverse SDE for y_t given by the equation

$$dy_t = [f(t)y_t + \frac{g(t)^2}{\sigma_t^2}(y_t - \alpha_t \mathbb{E}[y|x_t])]dt + g(t)d\bar{w}.$$

We recognize a an Ornstein-Uhlenbeck process with time-dependent parameters, which can be solved using the method of variation of constants. Considering that

$$f(t) + \frac{g(t)^2}{\sigma_t^2} = \frac{d}{dt} \log\left(\frac{\sigma_t^2}{\alpha_t}\right),$$

the SDE can the be written as

$$dy_t = \frac{d}{dt} \log\left(\frac{\sigma_t^2}{\alpha_t}\right) y_t dt - 2\frac{d}{dt}(\log\left(\frac{\sigma_t}{\alpha_t}\right)) \alpha_t \mathbb{E}[y|x_t] dt + g(t)d\bar{w}.$$

Since $\frac{\sigma_t^2}{\alpha_t}$ is a solution to the associated homogeneous equation, we apply Ito's formula to the function $\phi(t, y_t) = y_t \frac{\alpha_t}{\sigma_t^2}$ and get

$$\begin{aligned} y_T \frac{\alpha_T}{\sigma_T^2} - y_\tau \frac{\alpha_\tau}{\sigma_\tau^2} &= \int_\tau^T \frac{\alpha_t}{\sigma_t^2} dy_t + \int_\tau^T \frac{d}{dt} \left(\frac{\alpha_t}{\sigma_t^2}\right) y_t dt \\ &= \int_\tau^T \frac{\alpha_t}{\sigma_t^2} \left(\frac{d}{dt} \log\left(\frac{\sigma_t^2}{\alpha_t}\right) y_t dt - 2\frac{d}{dt}(\log\left(\frac{\sigma_t}{\alpha_t}\right)) \alpha_t \mathbb{E}[y|x_t] dt + g(t)d\bar{w}\right) + \int_\tau^T \frac{d}{dt} \left(\frac{\alpha_t}{\sigma_t^2}\right) y_t dt \\ &= \int_\tau^T \frac{d}{dt} \left(\frac{\alpha_t^2}{\sigma_t^2}\right) \mathbb{E}[y|x_t] dt + \int_\tau^T \frac{\alpha_t}{\sigma_t^2} g(t) d\bar{w}. \end{aligned}$$

Considering that $\alpha_T = 0$, we get

$$y_\tau = -\frac{\sigma_\tau^2}{\alpha_\tau} \int_\tau^T \frac{d}{dt} \left(\frac{\alpha_t^2}{\sigma_t^2}\right) \mathbb{E}[y|x_t] dt - \frac{\sigma_\tau^2}{\alpha_\tau} \int_\tau^T \frac{\alpha_t}{\sigma_t^2} g(t) d\bar{w}.$$

We remark that the stochastic term, which we note S_τ , converges almost surely to zero as τ converges to zero considering that the associated quadratic variation

$$\mathbb{E}[S_\tau^2] = \int_\tau^T \frac{\sigma_\tau^4}{\alpha_\tau^2} \frac{\alpha_t^2}{\sigma_t^4} g(t)^2 dt = \int_\tau^T \frac{\sigma_\tau^4}{\sigma_t^4} \frac{\alpha_t^2}{\alpha_\tau^2} \left(\frac{d\sigma_t^2}{dt} - 2\frac{d\alpha_t}{dt} \sigma_t^2\right) dt$$

converges to zero since $\sigma_0 = 0$ and $\alpha_0 = 1$.

Concerning the first term, we observe that it only depends on the behavior of $\mathbb{E}[y|x_t]$ near $t = 0$. Writing $\mathbb{E}[y|x_t] = \mathbb{E}[y|x_0] + \epsilon(t)$, this expression becomes

$$-\frac{\sigma_\tau^2}{\alpha_\tau} \int_\tau^T \frac{d}{dt} \left(\frac{\alpha_t^2}{\sigma_t^2} \right) \mathbb{E}[y|x_0] dt - \frac{\sigma_\tau^2}{\alpha_\tau} \int_\tau^T \frac{d}{dt} \left(\frac{\alpha_t^2}{\sigma_t^2} \right) \epsilon(t) dt .$$

The first term converges to $\mathbb{E}[y|x_0] = \mu(x_0)$ and the second term converges to zero since

$$\int_\tau^T \left| \frac{d}{dt} \left(\frac{\alpha_t^2}{\sigma_t^2} \right) \right| dt = \frac{\alpha_\tau^2}{\sigma_\tau^2} - \frac{\alpha_T^2}{\sigma_T^2} ,$$

and $\epsilon(t)$ converges to zero almost surely.

A.1.2 Proof of proposition 2 (ODE)

We consider the ODE for y_t

$$dy_t = [f(t)y_t + \frac{g(t)^2}{2\sigma_t^2}(y_t - \alpha_t \mathbb{E}[y|x_t])] dt ,$$

and have to show that starting from any value of y_T , this ODE leads to the value $y_0 = \mathbb{E}[y|x_0] = \mu(x_0)$. This ODE is a first order linear equation which can also be solved in integral form using the method of variation of constants:

We have

$$f(t) + \frac{g(t)^2}{2\sigma_t^2} = \frac{\dot{\sigma}_t}{\sigma_t} ,$$

and the ODE can then be written as:

$$\dot{y}_t = \frac{\dot{\sigma}_t}{\sigma_t} y - \frac{d}{dt} \left(\log \left(\frac{\sigma_t}{\alpha_t} \right) \right) \alpha_t \mathbb{E}[y|x_t] .$$

Considering that σ_t is a solution of the associated homogeneous equation, we get

$$\frac{d}{dt} \left(\frac{y_t}{\sigma_t} \right) = -\frac{\alpha_t}{\sigma_t} \frac{d}{dt} \left(\log \left(\frac{\sigma_t}{\alpha_t} \right) \right) \mathbb{E}[y|x_t] = \frac{d}{dt} \left(\frac{\alpha_t}{\sigma_t} \right) \mathbb{E}[y|x_t] ,$$

and

$$\frac{y_T}{\sigma_T} = \frac{y_\tau}{\sigma_\tau} + \int_\tau^T \left(\frac{d}{dt} \left(\frac{\alpha_t}{\sigma_t} \right) \right) \mathbb{E}[y|x_t] dt ,$$

which leads to

$$y_\tau = \frac{\sigma_\tau}{\sigma_T} y_T - \sigma_\tau \int_\tau^T \left(\frac{d}{dt} \left(\frac{\alpha_t}{\sigma_t} \right) \right) \mathbb{E}[y|x_t] dt .$$

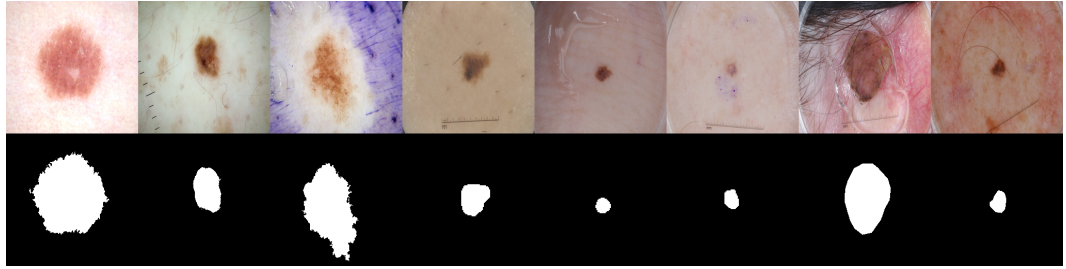
And we conclude by the same argument as for the SDE.

A.2 Dataset samples and generated samples

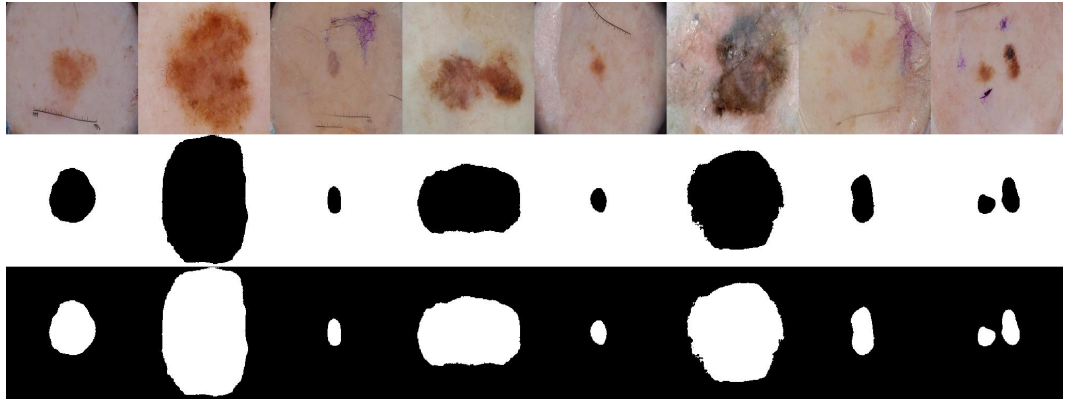
We provide below some samples of the datasets used in this paper as well as some generated samples for the datasets used for pretraining. The generated samples are created using trained hybrid diffusion models and the DPM-Solver ODE solver [26] implemented in the Hugging Face Diffusers framework with 100 inference steps. x_T values are sampled from a Gaussian normal distribution and all the y_T mask values are set to zero. The generated images shown are the direct outputs of the ODE solver. The generated masks shown are computed by selecting for each pixel the class with the higher mask value.

A.2.1 ISIC 2018 dataset

- Dataset samples

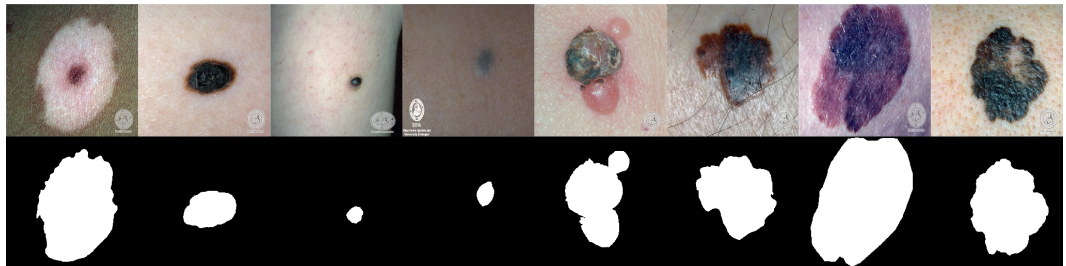


- Generated samples



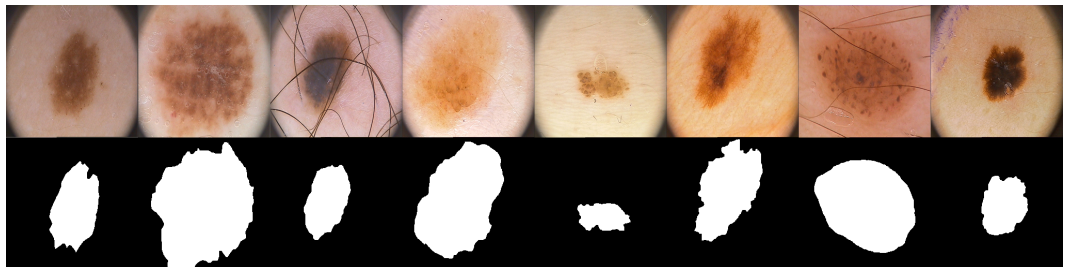
A.2.2 DermIS dataset

- Dataset samples



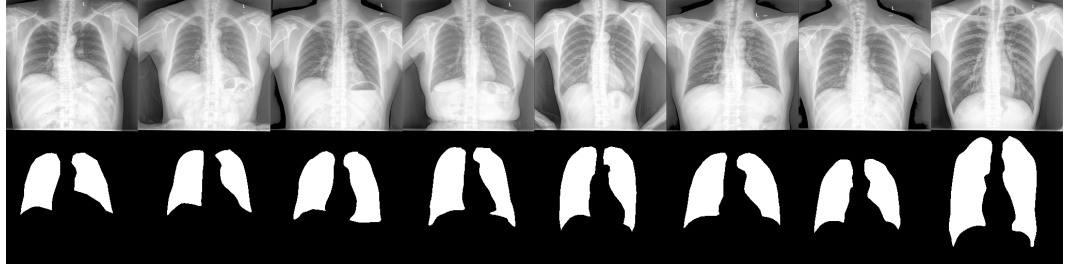
A.2.3 PH2 dataset

- Dataset samples:

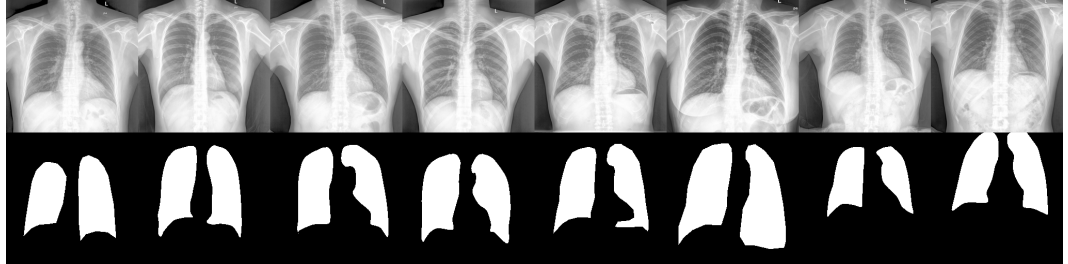


A.2.4 Shenzhen dataset

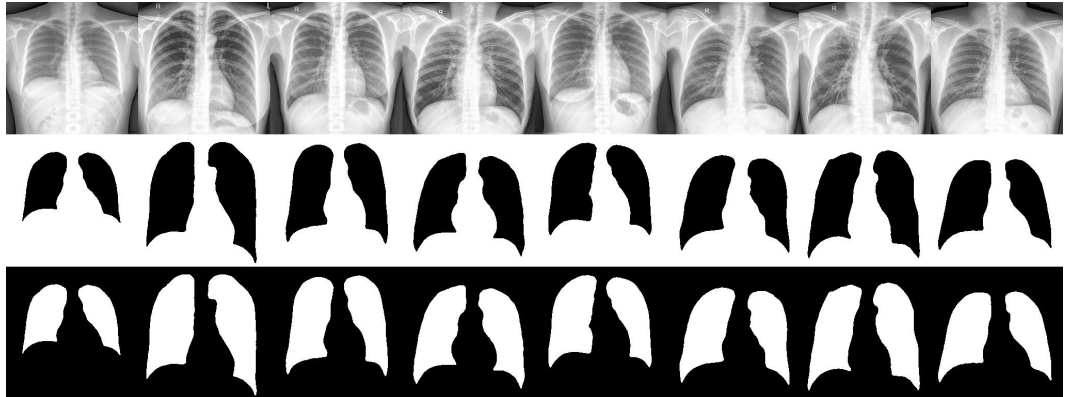
- Dataset samples (no data augmentation):



- Dataset samples (with data augmentation):

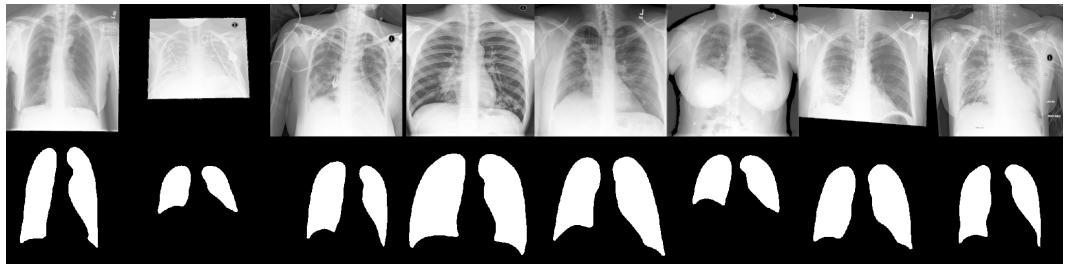


- Generated samples



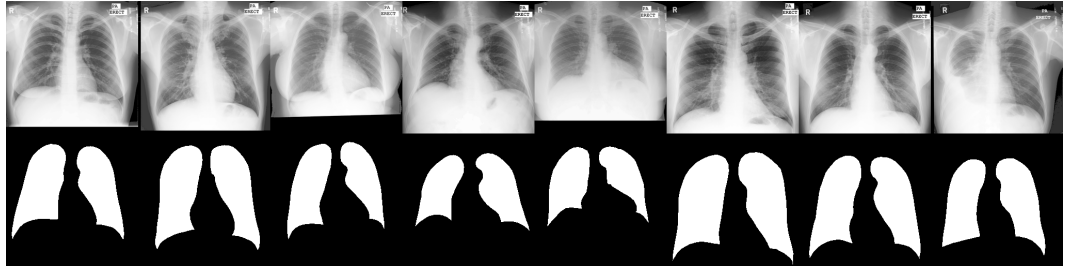
A.2.5 NIH dataset

- Dataset samples:



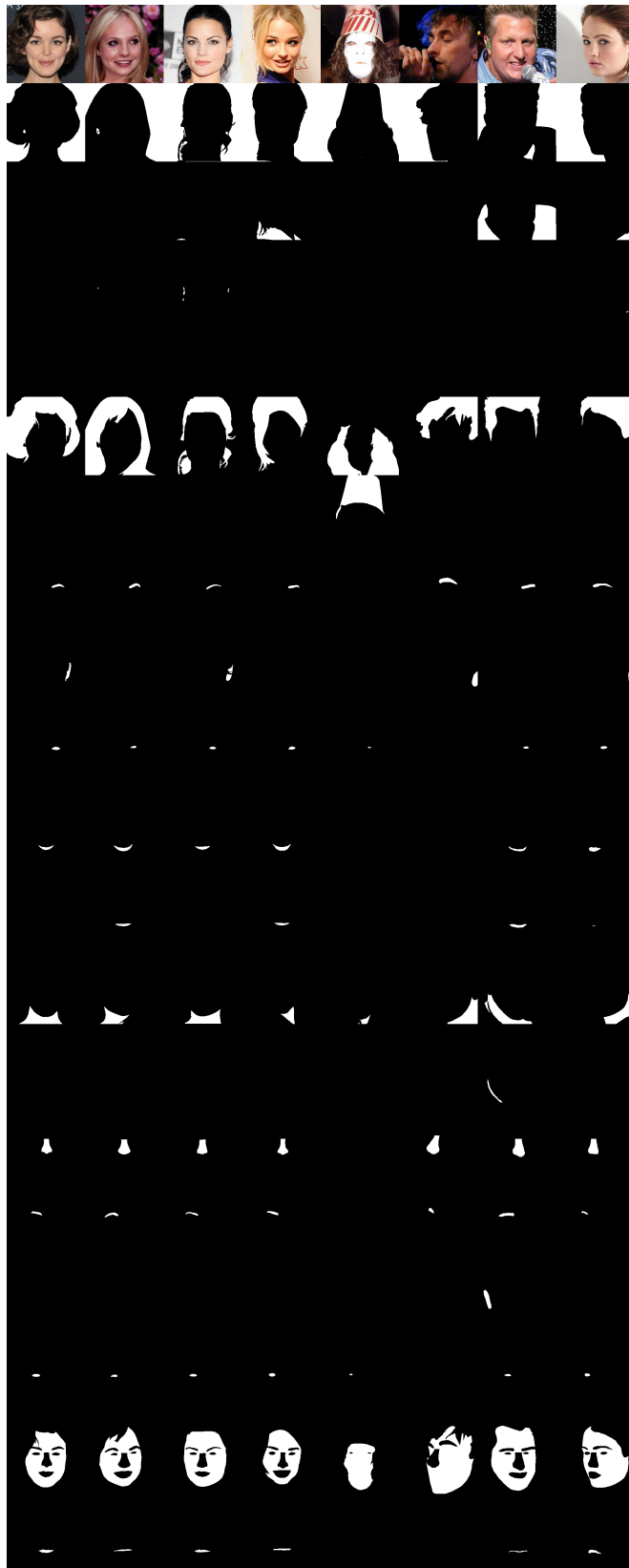
A.2.6 Montgomery dataset

- Dataset samples:

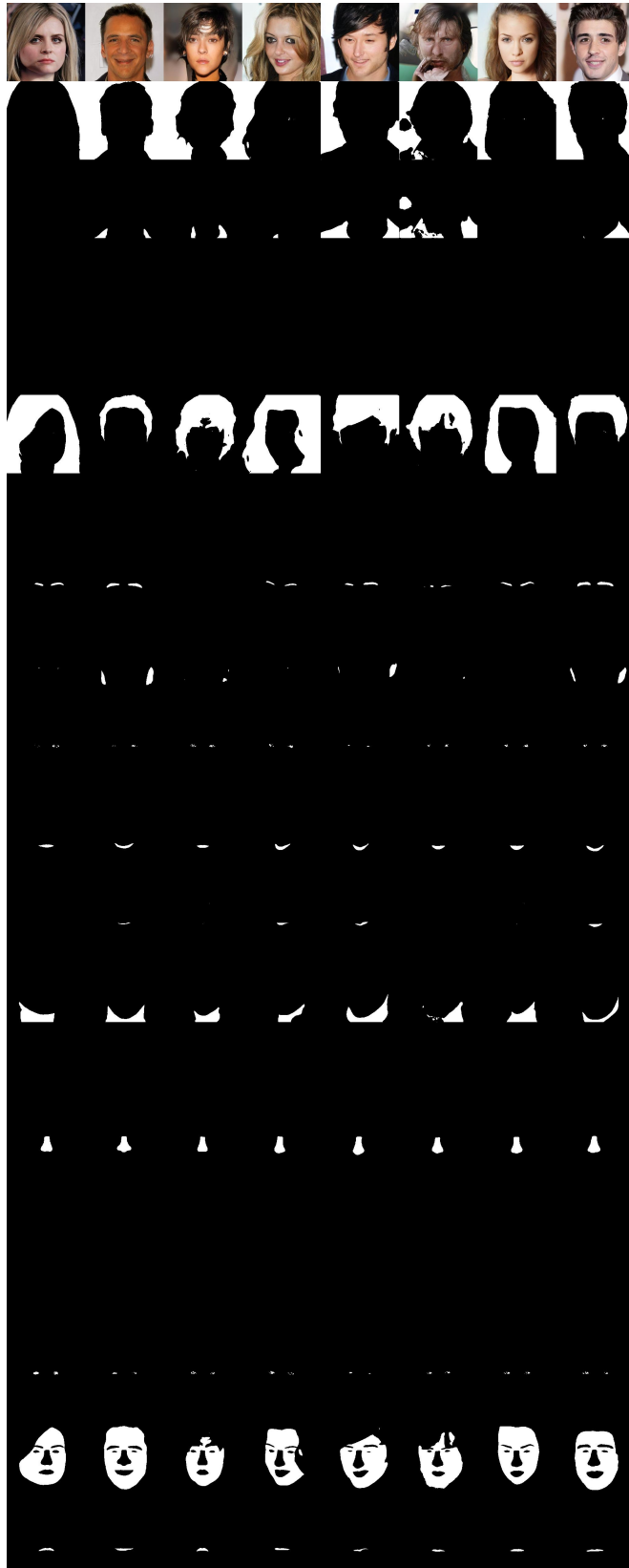


A.2.7 Celebamask-HQ dataset

- Dataset samples:



- Generated samples:



A.2.8 FFHQ-34 dataset

- Dataset samples:



A.3 Training and architecture details

The architecture of the ADM Unet is the same as in Dhariwal and Nichol [11], except for the number of model channels set to 128 instead of 256 and the number of output channels set at $3 + K$ where K is the number of classes. Chest X-ray black and white images (1 input channel) are converted to 3 channels images by duplicating the input channels. Pixel values are normalized to the range $[-1, 1]$ before being given to the Unet.

The full configuration settings of this ADM Unet in reproduced below for completeness:

- attention resolutions: [32,16,8]
- channel multipliers:[1,1,2,2,4,4]
- dropout : 0.1
- image size : 256
- number of input channels:3
- number of output channels:3+K
- number of model channels: 128
- number of head channels: 64
- number of residual blocks: 2
- resblock updown: true
- use fp16: false,
- use scale shift norm: true

We keep most of the default hyperparameters of the diffusers framework for training an unconditional diffusion model. We reproduce them below for completeness. It should be noted that since the time indexes associated to nonzero noises used in the diffusers framework are from 0 to 999 and not 1 to 1000, the fine-tuning is done with $t = 0$ and not $t = 1$.

- batch size: 64 for pretraining, 12 for fine tuning
- learning rate: 1e-4 for pretraining, 2e-4 for fine-tuning
- optimizer: AdamW
- Adam beta1: 0.95
- Adam beta2: 0.99
- Adam weight decay: 1e-6
- Adam epsilon: 1e-8
- number of warmup steps: 2000 for pretraining, 0 for fine-tuning
- Number of DDPM steps (T): 1000
- Schedule beta type: linear
- DDPM beta end: 0.02